GA-A--20094

DE91 002709

A SILICON AVALANCHE PHOTODIODE DETECTOR CIRCUIT FOR Nd:YAG LASER SCATTERING

by
C.L. HSIEH, J. HASKOVEC, T.N. CARLSTROM,
J.C. DeBOO, C.M. GREENFIELD, R.T. SNIDER,
and P. TROST

This is a preprint of a paper to be presented at the Eighth Topical Conference on High Temperature Plasma Diagnostics, May 7–10, 1990, in Hyannis, Massachusetts and to be printed in the *Proceedings.*

Work supported by
U.S. Department of Energy
Contract DE-AC03-89ER51114

GENERAL ATOMICS PROJECT 3466
JUNE 1990

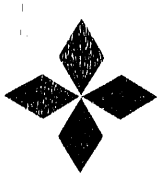

GENERAL ATOMICS

ABSTRACT

A silicon avalanche photodiode with an internal gain of about 50 to 100 is used in a temperature controlled environment to measure the Nd:YAG laser Thomson scattered spectrum in the wavelength range from 700 to 1150 nm. A charge sensitive preamplifier has been developed for minimizing the noise contribution from the detector electronics. Signal levels as low as 20 photoelectrons ($S/N = 1$) can be detected. Measurements show that both the signal and the variance of the signal vary linearly with the input light level over the range of interest, indicating Poisson statistics. The signal is processed using a 100 ns delay line and a differential amplifier which subtracts the low frequency background light component. The background signal is amplified with a computer controlled variable gain amplifier and is used for an estimate of the measurement error, calibration, and Z_{eff} measurements of the plasma. The signal processing has been analyzed using a theoretical model to aid the system design and establish the procedure for data error analysis.

INTRODUCTION

We describe a silicon avalanche photodiode (APD)[1] based detector system to be used in the multipulse Thomson scattering diagnostic now being built for DIII–D. The system will measure low level, short duration (10–15 nsec), light pulses from Nd:YAG laser light Thomson scattered by the tokamak plasma.

By low level light, we mean the photons in the light pulse may number less than 100. The detection of such a light pulse must be made in the presence of thermal (Johnson) noise associated with room temperature operation, and other noise sources, such as shot noise and amplifier noise.

These light pulse measurements must also be made in the presence of the continuous emission of background light, including plasma bremsstrahlung radiation and thermal radiation from the vessel walls. The background light has been measured on DIII–D to reach levels that would play a dominant role in the error analysis of the pulsed light measurement. Therefore, it is important to include this measurement when estimating the error of the pulsed light signal.

Silicon avalanche photodiodes (internal gain=100) are the only practical choice of detector for measuring Thomson scattering light from Nd:YAG lasers at 1064 nm. The long wavelength end of the measurable Thomson spectrum is limited by the silicon energy band gap which increases with decreasing temperature.[1,2] As a result, the detector quantum efficiency decreases with decreasing temperature and it is necessary for the detector to be operated at approximately room temperature to compromise between thermal noise and quantum efficiency. Theoretical estimates (see Appendix A) indicate that thermal noise at room temperature limits the sensitivity of APD to about 15 photoelectrons. A stable temperature must also be maintained to keep the drifts in detector responsivity to a minimum.

The expected signal levels cover a wide range. The total Thomson scattered signal is proportional to the electron density of the plasma, and the system should measure densities from 2×10^{18} to 2×10^{20} m^{-3}. The background light level may vary

as the square of this range, resulting in a range of 10^4. Since digitizers are frequently limited to a range of 10^3, some flexibility in the system gain is desired.

Our plan for a high spatial resolution profile measurement calls for over 300 detector electronics modules to be built. Therefore, the design is influenced not only by performance requirements, but also by cost considerations, production and test procedures, calibration and maintenance.

I. DETECTOR ELECTRONICS DESIGN

We have elected to utilize shaping of the fast pulse signal prior to the usual procedure of using fast gated integrators to sample the signal. Commonly, the pulse is made to fit entirely within the gate width of the integrators. In order to minimize the error contribution due to the background, the gate width is made as short as possible. In practice, the rise time of the amplifiers and the short dead time of the integrator after receiving a gate trigger must be considered in determining the actual gate width.

The optimal choice for the pulse shape (decay time) in relation to the gate width is less clear. We have modeled (Appendix A) the effect of a long decay time of the pulse (several times longer than the gate time) and found that the long decay time can actually improve the signal-to-noise ratio with respect to the noise caused by the presence of background light. This result is caused by the cross correlation between the two successive gates which sample the background signal twice. A long decay time is advantageous since it reduces the high frequency requirement of the electronic components, and allows more flexibility in the electronics design. However, the frequency limit of the amplifier must stay sufficiently high so the pulse signal will not be contaminated by variations of the background signal. For our application, a decay time to gate width ratio of about three was selected to give the best overall compromise.

Low noise, high speed op-amps are readily available and are relatively straight forward to incorporate in electronic design. Because of this, we have chosen to use op-amps rather than develop an electronic design with discrete components. Figure 1 shows the schematic of the circuit. The operational amplifiers were carefully chosen for their noise performance and gain-bandwidth product. The first op-amp sets the electronic noise level of the circuit and a Harris 5147 was selected for this application. The second op-amp provides additional gain and buffers the first amp from the delay line and the variable gain switches. A jumper is provided to reduce the gain by two if needed.

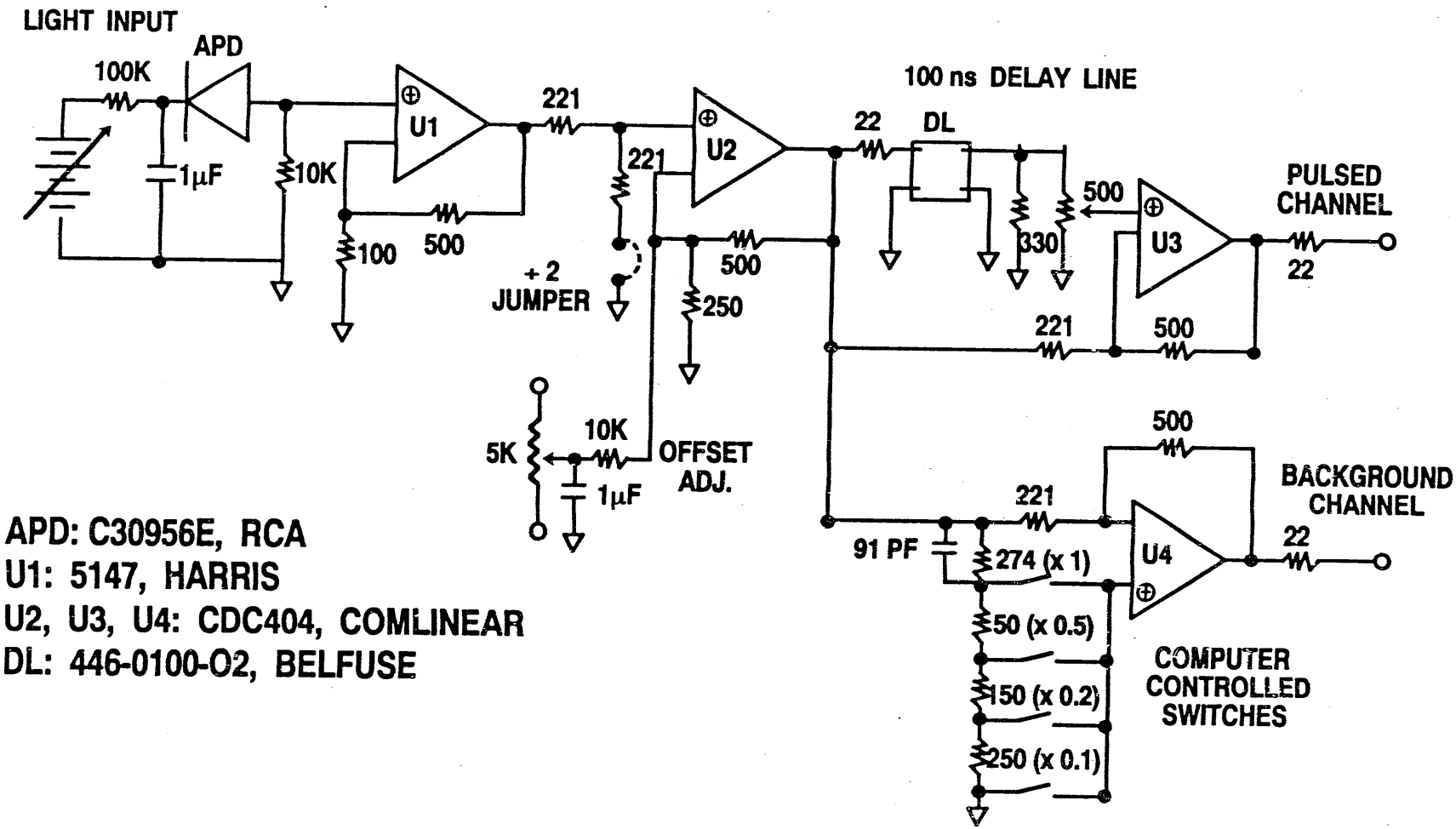

Fig. 1. Circuit diagram of detector electronics.

The pulse channel output is formed using a delay line technique[3] which subtracts a signal delayed by 100 nsec from a non-delayed signal. The chief advantage of the delay line technique is to allow the full digitizer range to be utilized for the pulsed light measurement alone. The variable resistor at the output of the delay line is used to properly balance the differential stage for zero output at zero frequency. The performance of the circuit in terms of the rejection ratio of low frequency signal is shown in Fig. 2. Figure 3 shows traces of the pulse and background channel response to a 15 ns light pulse along with the integrator gates. The gain of the background channel can be changed over a range of 10 by a set of computer controlled switches. The switches are placed in a portion of the circuit that has very little current so that the internal impedance of the switches does not affect performance.

Because the background channel is dc coupled throughout the entire circuit and it has the same pulse response as the pulse channel during the integrator gate, the detector electronics assembly can be calibrated using dc light sources. This offers a significant advantage over circuits that only measure pulsed light. There is a difference in the dc and pulsed gain of the circuit, however, but this can be calibrated independently.

Due to concern over the thermal stability of the detector, the APD is placed in a separate chamber away from the circuit board, and the detector electronics assembly is arranged to sink heat to a water cooled polychromator frame structure.[4]

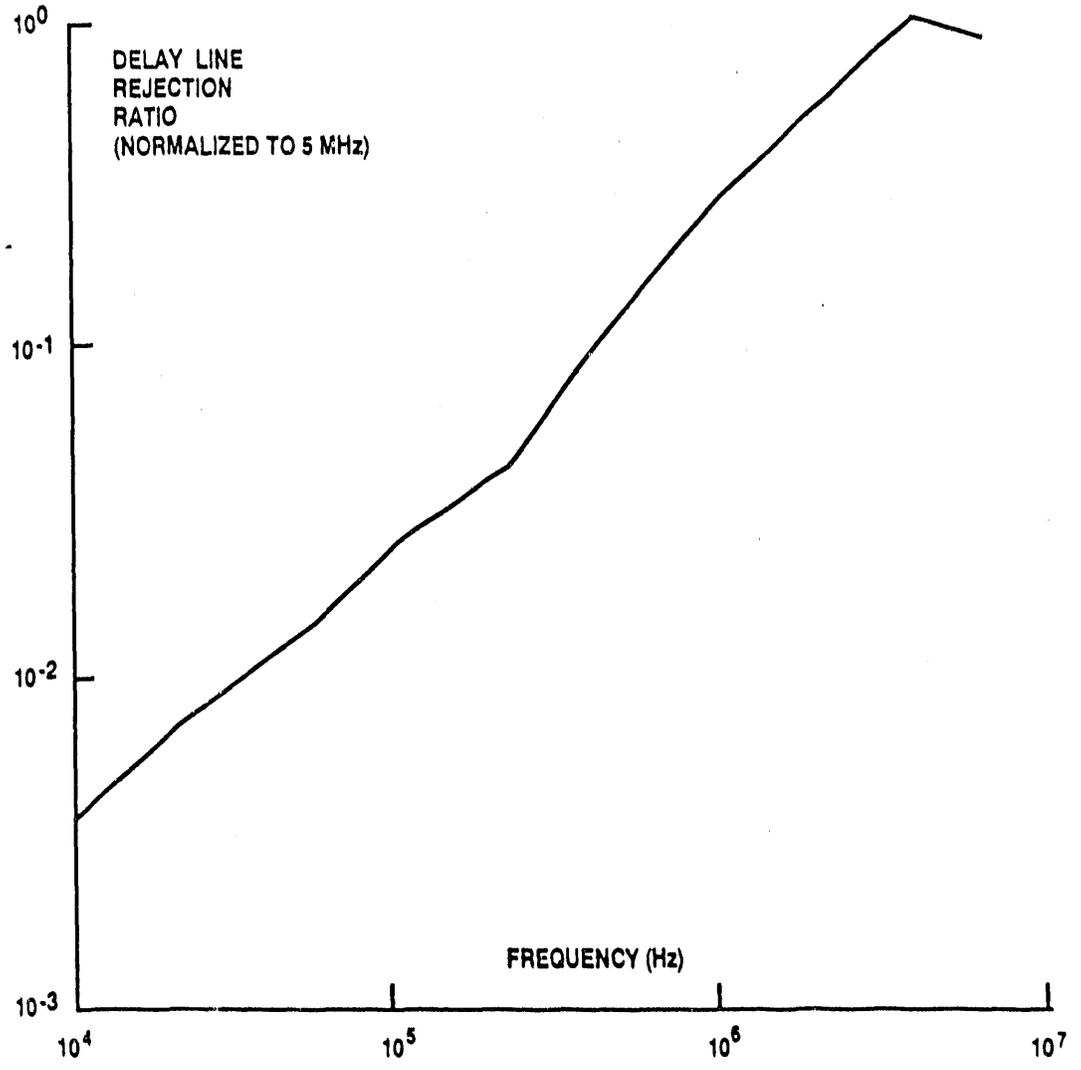

Fig. 2. Delay line rejection ratio of the pulse channel as a function of frequency.

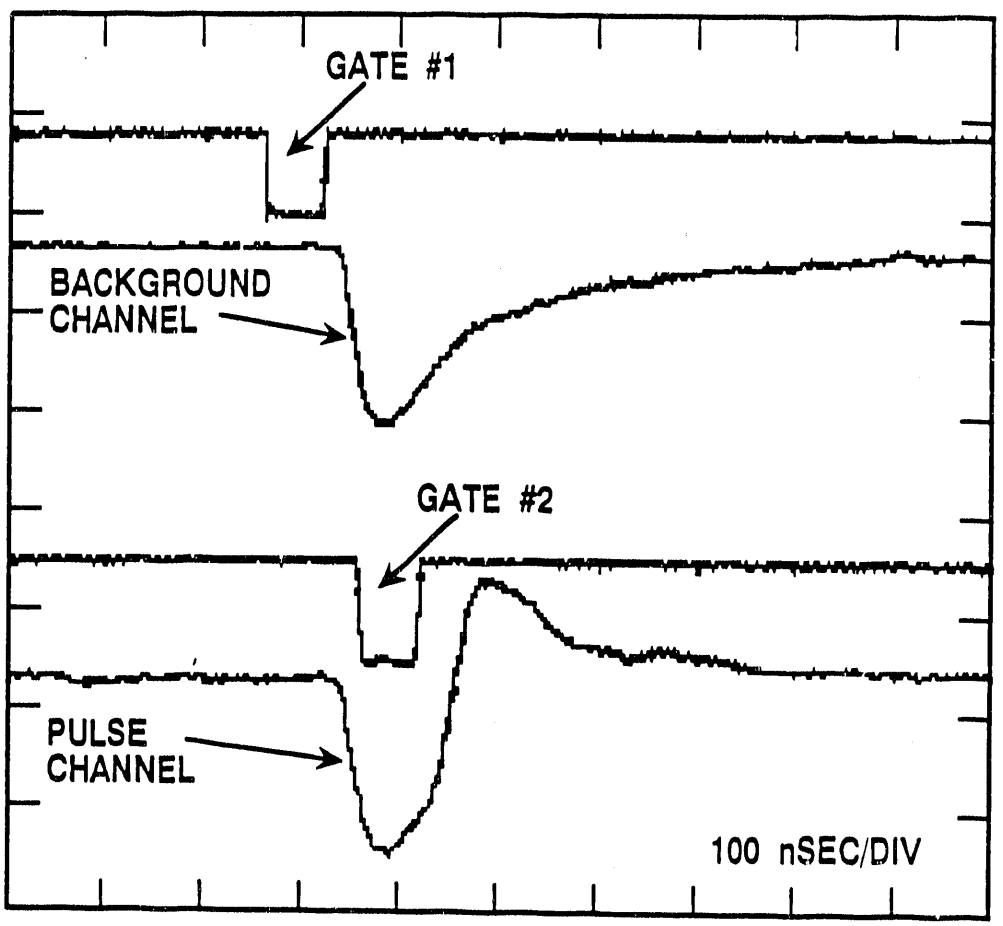

Fig. 3. Oscilloscope traces showing the response of the pulse and background channels to a 15 ns light pulse along with the two integrator gates.

II. TEST RESULTS

Monochromatic sources of both dc and pulsed light are used in the test measurements, and the source light intensity is monitored using an EG&G Model 690 radiometric detector standard of a recent, traceable calibration. For each data point, we obtain 1000 samples in order to calculate the average signal and the variance. The variance measurement can be misleading because of instrumental fluctuation. Therefore, it is necessary that all significant sources of fluctuation be found and accounted for. For example, the HeNe laser used for the dc source had a 0.5% fluctuation level, and the pulsed light source had a 1.6% fluctuation level. Although small, these levels can lead to significant measurement errors of the signal variance. Figure 4 shows that both the signal (average integrator counts) and the signal variance (dark variance excluded) vary linearly with the input light level, demonstrating that the system is linear and follows the photoelectron statistics. The curves in the figure are calculated from our model using measured gains and excessive noise factor.

Measurements were performed using a pulsed light source to determine the number of photoelectrons Q_1 required for having S/N = 1. Figure 5 shows a plot of Q_1 as a function of the APD bias voltage. Q_1 decreases with increasing bias voltage until a minimum of less than 20 photoelectrons is reached. At higher voltage, near avalanche breakdown, Q_1 increases.

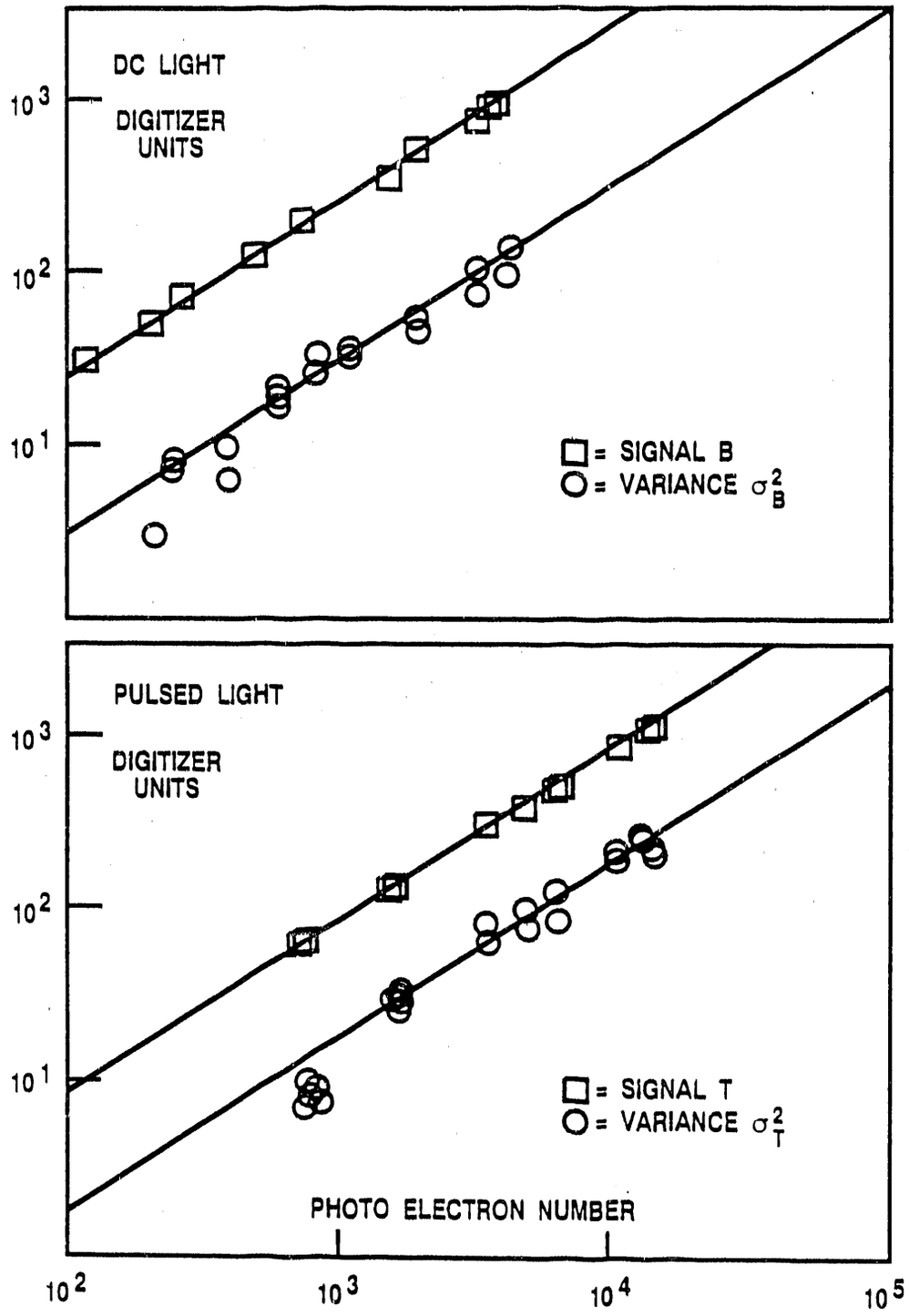

Fig. 4. Response and variance of detector circuit as functions of photoelectron count. The solid lines are calculated using the measured gains and excessive noise factor. (a) dc light measured on background channel, (b) pulsed light measured on pulse channel.

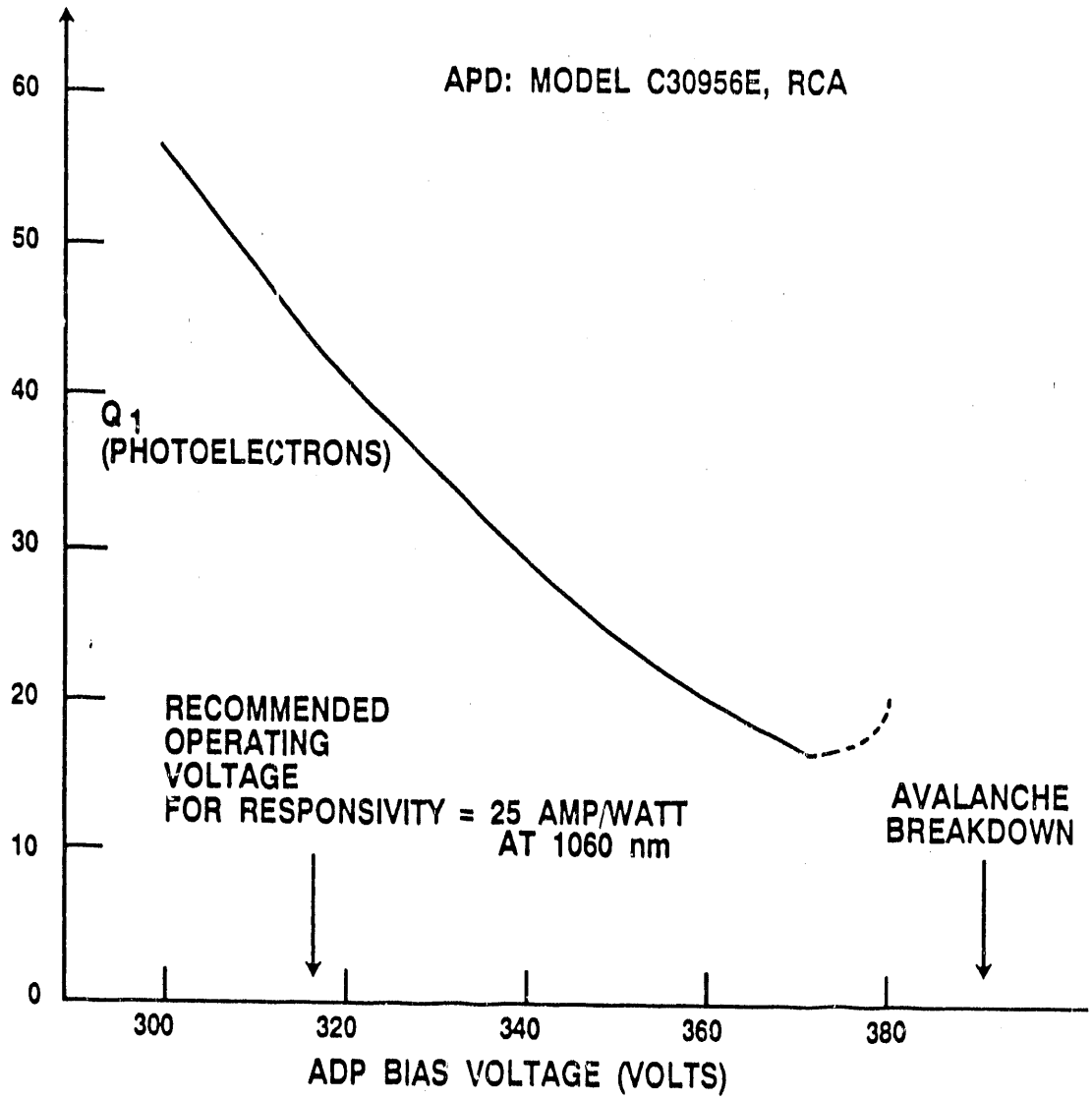

Fig. 5. Minimum detectable number of photoelectrons ($S/N = 1$) as a function of APD bias voltage.

REFERENCES

[1] P. P. Web, R. J. McIntyre, and J. Conradi, RCA Review **35**, 234 (1974).

[2] S. M. Sze, in *Physics of Semiconductor Devices*, (John Wiley & Sons, New York, 1969), pp. 24 and 54.

[3] A. Bregni and L. Giudicotti, J. Phys. E: Sci. Instrum. **15**, (1982).

[4] T. N. Carlstrom et al., this conference, (1990).

ACKNOWLEDGMENT

The authors are pleased to acknowledge G. Campbell and E. McKee for their help at various stages of this work, and to thank J. Land for his effort in coordinating the mass production and assembly of the detector electronics modules. This work was supported by the U.S. Department of Energy under Contract No. DE-AC03-89ER51114.

APPENDIX A

A.I. ESTIMATE OF THE THERMAL NOISE

As a convenient reference for noise comparisons, we can calculate the signal level which equals the thermal (Johnson) noise of the APD circuit shown in Fig. A1(a). The condition for the square of the voltage across the diode due to light to equal the square of the thermal noise voltage of the load resistor (summing over all frequencies) can be written as

$$\left(\frac{M\,Q_T\,e}{C}\right)^2 = \int_0^\infty \frac{4\,k\,T_F\,R_F\,df}{1+(2\,\pi f)^2\,R_f^2\,C^2} = \frac{k\,T_F}{C} \quad , \tag{A.1}$$

where Q_T is the photoelectron number, $C = C_D + C_E$ is the sum of diode and external capacitances, M is the diode avalanche multiplication gain, and T_F is the temperature of the load resistor R_F. As indicated in the righthand side of Eq. (A.1), the total noise energy, frequently known as the KTC noise,[A1] is independent of the resistor value. The required photoelectron number Q_T is given by

$$Q_T = \frac{1}{M\,e}\,(k\,T_F\,C)^{1/2} \simeq 15 \text{ photoelectrons} \quad , \tag{A.2}$$

where a specific APD (RCA model C30956E, 3 mm diam., 10 pF, and $M = 100$), $C_E = 5$ pF and room temperature are assumed. The number Q_T is a lower limit (for a broad band application) and a convenient reference for noise comparison. Despite their low cost and other advantages, silicon photodiodes (internal gain=1) do not

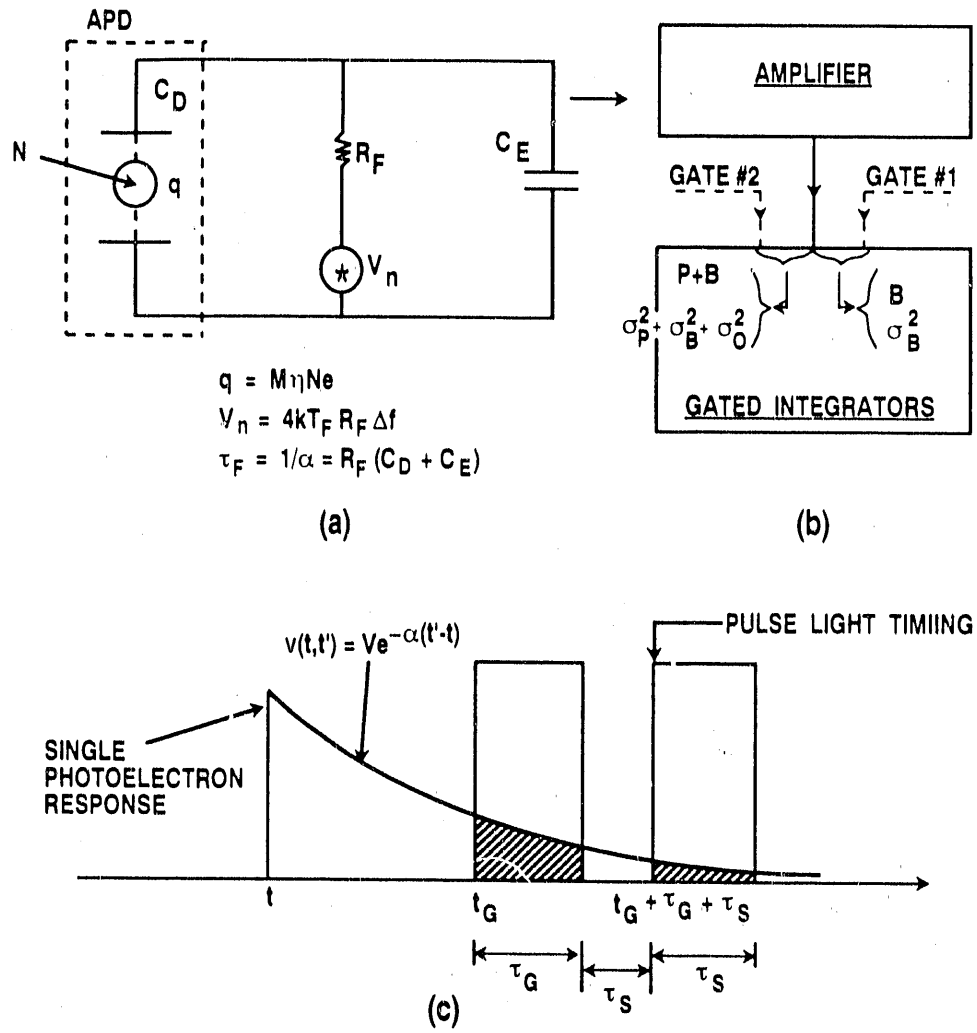

Fig. A1. Simplified diagrams: (a) the APD load circuit, (b) the block arrangement of the detector electronics, (c) the timing arrangement of the integrator gates and a single photoelectron voltage waveform.

have the necessary sensitivity for this application due to thermal noise considerations alone.

A.II. SIGNAL PROCESSING MODEL

We have developed a model to aid our understanding of the detector system, predict consequences of design choices, and analyze performance. We are particularly interested in how to calculate and minimize the error of the pulsed light measurement. A simplified schematic of the APD, the amplifier, and gated integrator (digitizer) is

shown in Fig. A1(a) and A1(b). Two integrators, gated for time τ_G, are used to sample the amplifier output, one for the background signal and the other for the combined signal. A temporal diagram of the response of the circuit to a single photoelectron and the time the integrators are active are shown in Fig. A1(c). The corresponding integrated signals (in counts) are B and $(P+B)$. Subtraction of the two integrated signals gives the Thomson light information T and its variance as

$$T = (P+B) - B = P \quad , \tag{A.3}$$

$$\sigma_T^2 = \sigma_P^2 + 2\,\sigma_B^2 - 2\,\sigma_{B12}^2 + \sigma_0^2 \quad , \tag{A.4}$$

where σ_{B12}^2 is the cross correlation term of the background between the two gates, and σ_0^2 is the variance of the pulse channel with no light input (dark variance) to be determined by test measurements.

For a single photoelectron generated at time t, we assume the response current at time t' at the integrator is given by

$$i(t,t') = I\,e^{-\alpha(t'-t)} \quad , \tag{A.5}$$

where I is the instantaneous response of the circuit, $\alpha = 1/\tau_F$ and $\tau_F = R_F(C_D + C_E)$, as shown in Fig. 1. Let $r(t)$ be the photoelectron birth rate due to the background light. The background signal count B and its variance σ_B^2 can be written as

$$B = \int_{-\infty}^{t_G} Ca(t)\,r(t)\,dt + \int_{t_G}^{t_G+\tau_G} Cb(t)\,r(t)\,dt \quad , \tag{A.6}$$

$$\sigma_B^2 = F \times \left[\int_{-\infty}^{t_G} C^2\,a^2(t)\,r(t)\,dt + \int_{t_G}^{t_G+\tau_G} C^2\,b^2(t)\,r(t)\,dt\right] \quad , \tag{A.7}$$

where C is a constant of the integrator, $F = \langle M^2 \rangle / \langle M \rangle^2$ is the excessive noise factor resulting from the probability distribution of multiplication in the APD, and

$$c(t) \equiv \int_{t_G}^{t_G+\tau_G} i(t,t')dt' \text{ and } b(t) \equiv \int_{t}^{t_G+\tau_G} i(t,t')dt' \quad ,$$

are the contributions of a single photoelectron generated either before or during a gate.

Since a single photoelectron response may contribute to both gates, there is cross correlation σ^2_{B12} between the two measurements which can be expressed as

$$\sigma^2_{B12} = \int_{-\infty}^{t_G} C^2\, a(t)\, c(t)\, r(t)\, dt + \int_{t_G}^{t_G+\tau_G} C^2\, b(t)\, c(t)\, r(t)\, dt \quad , \qquad \text{(A.8)}$$

where

$$c(t) \equiv \int_{t_G+\tau_G+\tau_S}^{t_G+2\,\tau_G+\tau_S} i(t,t')dt'$$

is the contribution to the second gate by photoelectrons generated before or during the first gate, and τ_S is the time separation between the two gates.

If Q_P photoelectrons are instantaneously introduced at the beginning of the second gate, the pulsed light contribution and variance can be written as

$$P = \int_{t_G+\tau_G+\tau_S}^{t_G+2\,\tau_G+\tau_S} Q_P\, C\, i(t)dt \quad , \qquad \text{(A.9)}$$

$$\sigma^2_P = F \int_{t_G+\tau_G+\tau_S}^{t_G+2\,\tau_G+\tau_S} Q_P\, C^2\, i^2(t)dt \quad . \qquad \text{(A.10)}$$

We can evaluate these equations for a constant background rate R_B. The overall gain of the background (in counts per photoelectron) can be written as $G_B = CI\tau_F$. The pulsed light gain is different from the background gain because the Q_P photoelectrons for the pulsed light are all introduced at the beginning of the gate and not

distributed in time like the background. The pulsed light channel gain is $G_P = yG_B$, where $y = 1 - e^{-x}$ and $x = \tau_G / \tau_F$.

Using the above substitutions, the equations can be evaluated and are summarized below,

$$T = P = G_P Q_P \quad , \qquad \sigma_P^2 = F G_P^2 Q_P \quad , \tag{A.11}$$

$$B = G_B \tau_G R_B \quad , \qquad \sigma_B^2 = F G_B^2 \tau_G R_B \left(1 - \frac{y}{x}\right) \quad , \tag{A.12}$$

$$\sigma_{B12}^2 = F G_B^2 \tau_G R_B \left(\frac{y^2 e^{-\alpha \tau_S}}{2x}\right) \quad , \tag{A.13}$$

Not surprisingly, Eq. (12)1 tells us that to minimize the error contribution due to the background, τ_G should be made as short as possible. In practice, the rise time of the amplifiers and the short dead time of the integrator after receiving a gate trigger must be considered in determining the actual τ_G. The optimal choice of τ_F, the decay time of the pulse, in relation to τ_G is less clear. Evaluating the signal-to-noise ratio of the pulsed light measurement as a function of x we obtain

$$\frac{T}{\sigma_T} = \left(\frac{Q_P}{F \times \left\{\left[\frac{2(x-y)}{y^2} - e^{-\alpha \tau_S}\right] \frac{\tau_G R_B}{x Q_P} + 1\right\} + \frac{\sigma_0^2}{G_P^2 Q_P}}\right)^{1/2} \quad . \tag{A.14}$$

A plot of this equation is shown in Fig. A2 for a typical set of parameters. The variation of x over a wide range does not make a significant difference in T/σ_T. This is a result of the effect of the cross correlation term σ_{B12}^2. The net background contribution $(\sigma_B^2 - \sigma_{B12}^2)$ changes little as τ_F increases because the correlation between the two gates improves. A long decay time is advantageous since it reduces the high frequency requirement of the electronic components, and allows more flexibility in the

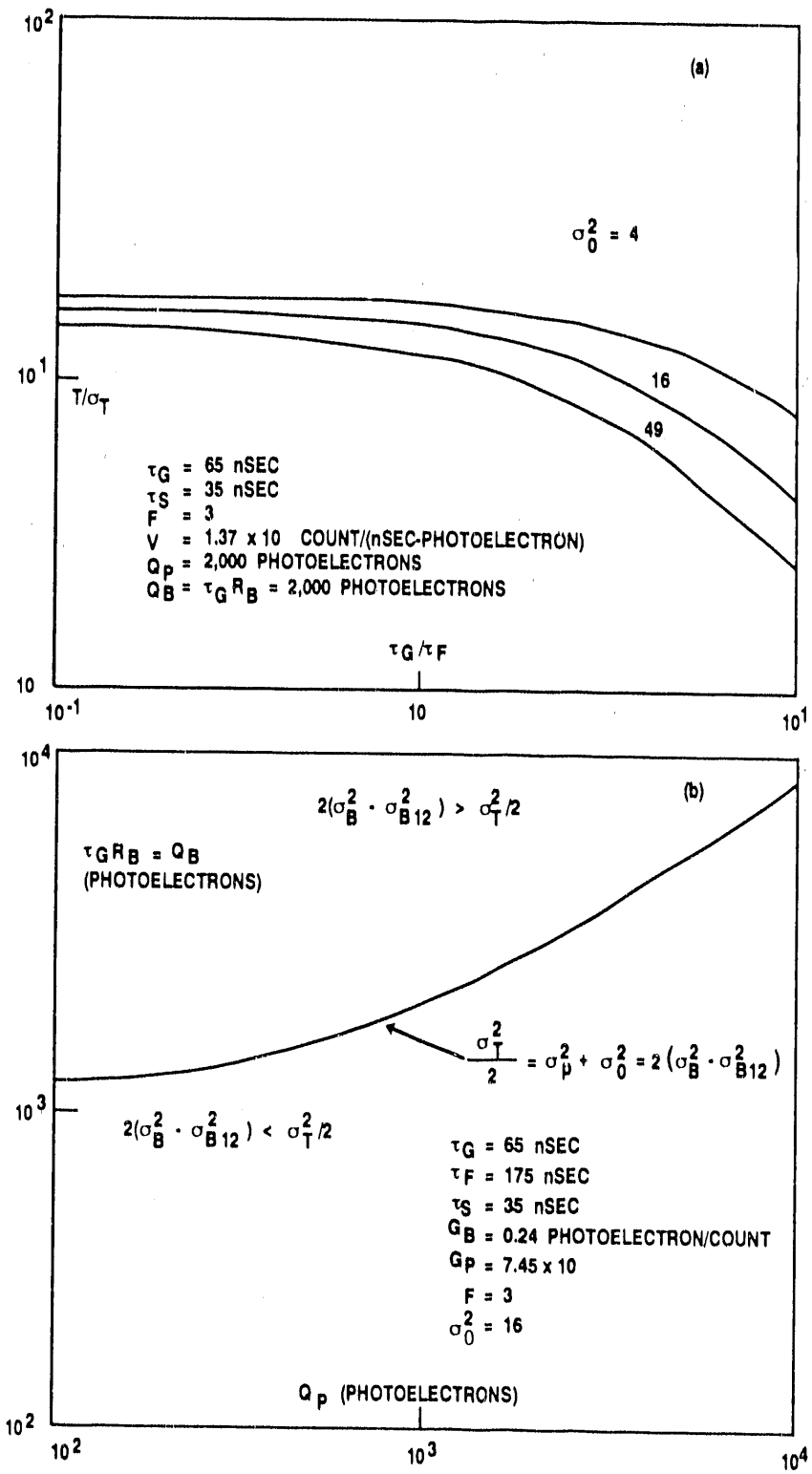

Fig. A2. Calculation result using the signal processing model showing the signal-to-noise ratio T/σ_T as a function of the ratio of the gate width to the decay time, $x = \tau_G/\tau_F$ for different values of the electronic noise, σ_0.

electronics design. However, the frequency limit of the amplifier must stay sufficiently high so the pulse signal will not be contaminated by variations of the background signal. T/σ_T decreases with shorter τ_F (large x) because a pulse width less than the gate width reduces the signal, whereas the dark variance contribution to σ_T^2 remains nearly constant.

REFERENCE

[A1] C. D. Motchenbacher and T. C. Fitchen, in *Low-Noise Electronics Design*, (John Wiley & Sons, New York, 1973), p. 23.

END

DATE FILMED

12/03/90